Customer	**:**	**ESRIN**	**Document Ref**	**:**	**IDEAS+-SER-IPF-REP-2992**
Contract No	**:**	**21525/08/I-OL**	**Issue Date**	**:**	**27 August 2018**
WP No	**:**	**xxxxx**	**Issue**	**:**	**1.0**

Title : **ERS-1 Scatterometer Full Mission Reprocessing Verification Report**

Abstract : This document presents the final verification report for the ERS-1 SCATT full mission reprocessing

Author : ____________________ D. Casella

Approval : ____________________ S. Pinori

Accepted : ____________________ P. Goryl

Distribution : **Hard Copy File:**
Filename: IDEAS+-SER-IPF-REP-2992_SCATT_ERS1_Full_Mission_Reproc_Report.doc

Telespazio VEGA UK Ltd
350 Capability Green, Luton, Bedfordshire, LU1 3LU, United Kingdom
Tel: +44 (0)1582 399 000 Fax: +44 (0)1582 728 656
www.telespazio-vega.com

Telespazio
A Finmeccanica/Thales Company

serco

TABLE OF CONTENTS

AMENDMENT POLICY

This document shall be amended by releasing a new edition of the document in its entirety. The Amendment Record Sheet below records the history and issue status of this document.

AMENDMENT RECORD SHEET

ISSUE	DATE	REASON
1.0	27/08/2018	First release

1. INTRODUCTION AND SUMMARY

The re-processing campaign of ERS-2 Scatterometer Level 2.0 products has been completed on 14/03/2015, adopting the latest Advanced Scatterometer Processing System (ASPS) version 10.04. Moreover on May 2018 these dataset have been enlarged with the re-processing campaign of ERS-1 Scatterometer Level 2.0 products. The present report summarized the quality control analysis performed about the radiometric calibration of the instrument and the monitoring of the instrument stability and of the wind products deviations with respect to the ECMWF model.

In each section results are shown for three kind of data:

- ERS-1 Operational data
- ERS-1 ASPS reprocessed data
- ERS-2 ASPS reprocessed data

This has been done in order to allow comparisons and to outline the net effect of the reprocessing of the ERS-1 dataset and for a first evaluation of the coherence between ERS-1 and ERS-2 re-processed datasets.

For the <u>calibration performance</u> the results are:

- The evolution of the maximum position of the gamma nought histograms computed over the rain forest is stable. On average the peak values for the aft and fore antenna are very close together, while for the mid antenna the peak value is roughly 0.2 dB less than the fore-aft case. A seasonal effect it also present in the peak position evolution for the three antennae.

- For the antenna patterns over the rain forest are flat within 0.3 dB for both ascending and descending passes.

For the <u>instrument performance</u> the results of the monitoring are:

- The reprocessing had no effect on the internal calibration level.

- The Doppler compensation was very stable for the full ERS-1 mission and the standard deviation is reduced from the operational ERS-1 dataset of a 50%.

- A stable performance in the noise power. During the full mission no instability has been detected in the noise power and in the internal calibration level.

For the <u>product performance</u> the results are:

- PCS quality control has reported stable results.

- The number of valid sigma-nought triplets is roughly 250,000 per day.

- The mean wind direction deviation is within -5, +5 degrees. The wind speed bias ranges from 0.0m/s to 1 m/s with a standard deviation smaller than 4 m/s.

2. CALIBRATION PERFORMANCES

The calibration performances are estimated using the South American rain forest as a vicarious calibration target. This approach allow us to design the correct calibration using an extended but noisy information from rain forest for which the main component of the variance comes from the geophysical evolution of the natural target.

The major goals of the calibration monitoring activities are the achievement of a “flat” antenna pattern profile and the assurance of a stable absolute calibration level.

2.1 Gamma-nought over Brazilian rain forest

The tropical rain forest in South America has been used as a reference distributed target. The target at the working frequency (C-band) of ERS-1 and ERS-2 Scatterometers acts as a very rough surface, and the transmitted signal is equally scattered in all directions (the target is assumed to follow the isotropic approximation). Consequently, for the angle of incidence used by ERS-1/2 Scatterometers, the normalised backscattering coefficient (sigma-nought) will depend solely on the surface effectively seen by the instrument:

$$S^0 = S \cdot cos\theta$$

With this hypothesis it is possible to define the following formula for the gamma-nought γ^0:

$$\gamma^0 = \frac{\sigma^0}{cos\theta}$$

Using this relation, the gamma-nought backscattering coefficient over the rain forest is independent of the incident angle, allowing the measurements from each of the three beams to be compared.

2.2 Definition of the target area

In order to define a convenient target area we have processed the ESA CCI Land cover classification map (http://www.esa-landcover-cci.org/ in the version 1.6.1) and we have selected the region within 15°S-13°N and 80°W-45°W. Figure 1 shows the ESA CCI land cover class map over the selected region. Then we have selected the pixels in the map corresponding with a land cover class “broadleaved evergreen tree” (class 50).

The ESA CCI land cover map has a spatial resolution of 300m while the ERS-1/2 scatterometers nominal resolution is about 25 km. In order to develop a target area taking into account the ERS scatterometer resolution we have applied a 2d normalized box filter (83 x 83) to the mask, in this way the original resolution was downgraded to about 25 km keeping the original fine sampled grid. The final target area representing the rain forest has been defined as the area where the application of the box filter gave a result higher than 0.95, in other terms the final target area is built from the pixels where the 95% of the neighbour pixels (within a box 25 km large centred on that pixel) have been classified as “broadleaved evergreen tree”. Figure 2 shows a map of the final target area.

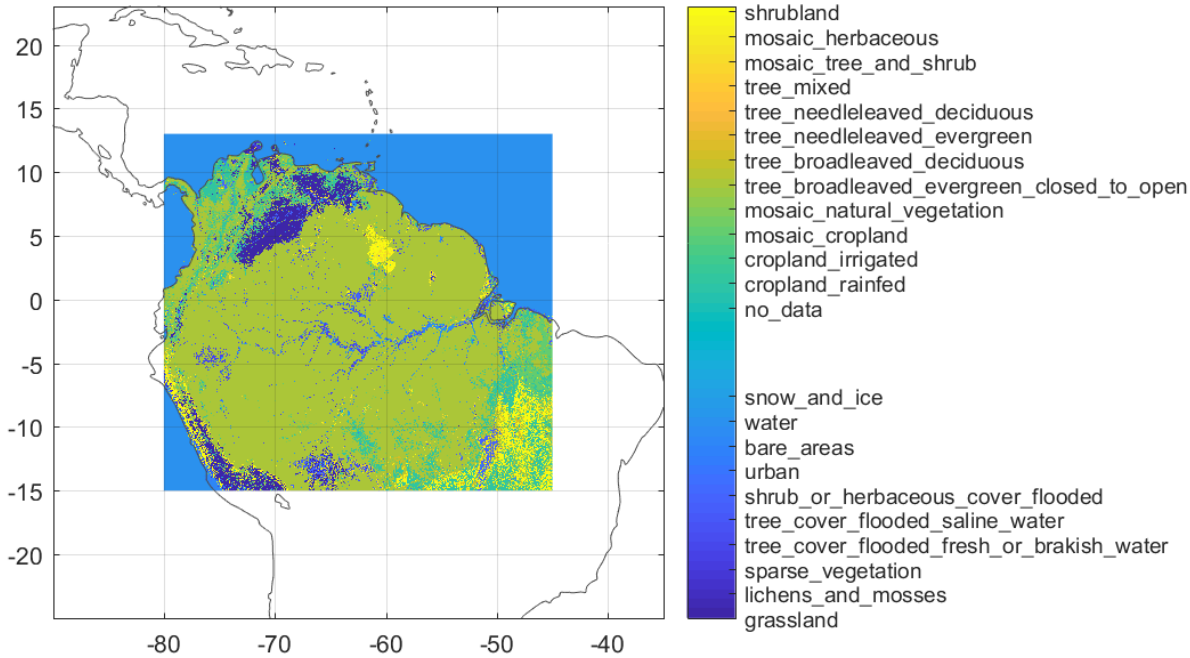

Figure 1 ESA CCI Land Cover Classification Map over the selected area in South America.

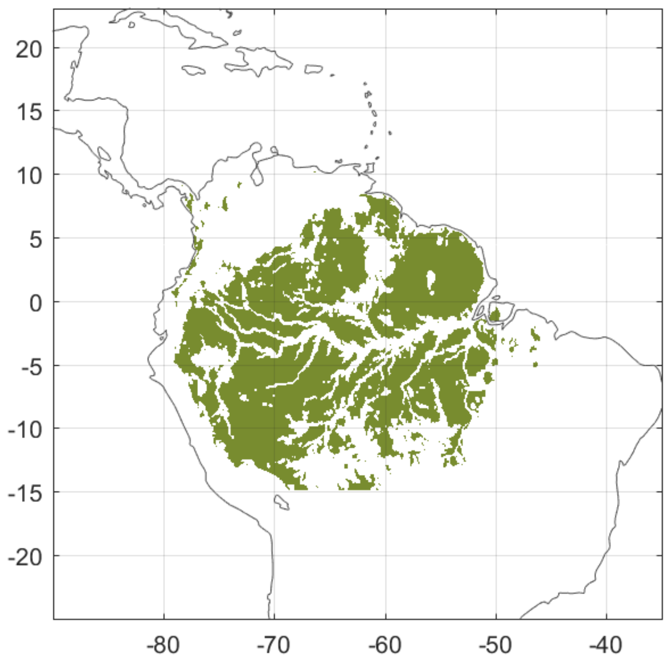

Figure 2 Final Target Area map

2.3 Gamma-nought histograms and peak position evolution

As the gamma-nought is independent from the incidence angle, the histogram of gamma-noughts over the rain forest is characterized by a sharp peak. The time-series of the peak position gives some information on the stability of the calibration. This parameter is computed by fitting the histogram with a normal distribution added to a second order polynomial

$$F(x) = A_0 exp\left(-\frac{z^2}{2}\right) + A_3 + A_4 x + A_5 x^2$$

Where:

$$z = \frac{x - A_1}{A_2}$$

The parameters are computed using the Levenberg-Marquardt nonlinear least squares algorithm. The position of the peak is given by the maximum of the function F(x). The histograms are computed weekly (from Monday to Sunday) for each antenna individually (“Fore”, “Mid”, and “Aft”) and for ascending and descending passage with a bin size of 0.02 dB, as it presented in Figure 3.

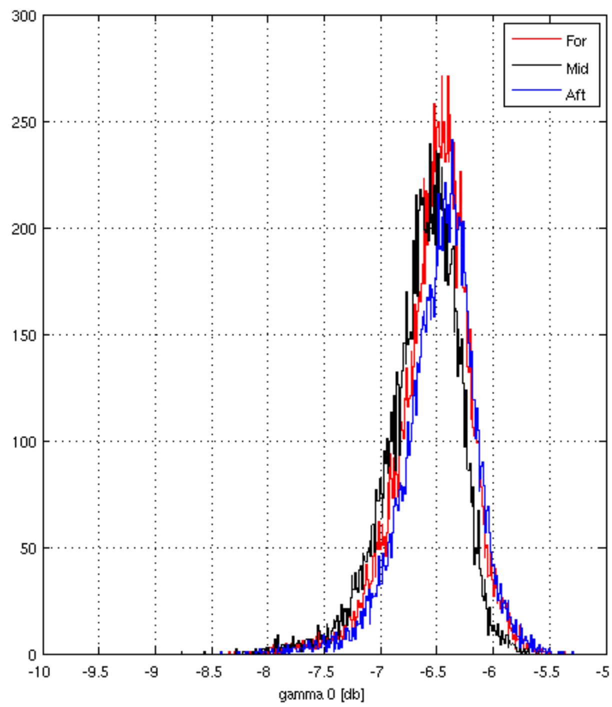

Figure 3 Example of a histogram of the Gamma0 over the rain forest, for ERS-1 ASPS reprocessed data during Cycle 156.

Figure 4 shows the evolution of the histograms peak position since August 1991 for the Ascending overpasses, a strong variability associated with a periodic annual variation is clearly visible, moreover some bias can be observed between the ASPS and the operational ERS-1 data especially for the After Beam. From the plots in Figure 4 it is clear that the calibration stability achieved over the rain forest is within 0.5 dB. On average the peak values for the aft and fore antenna are very close together, while for the mid antenna the peak value is roughly 0.2 dB less than the fore-aft case.

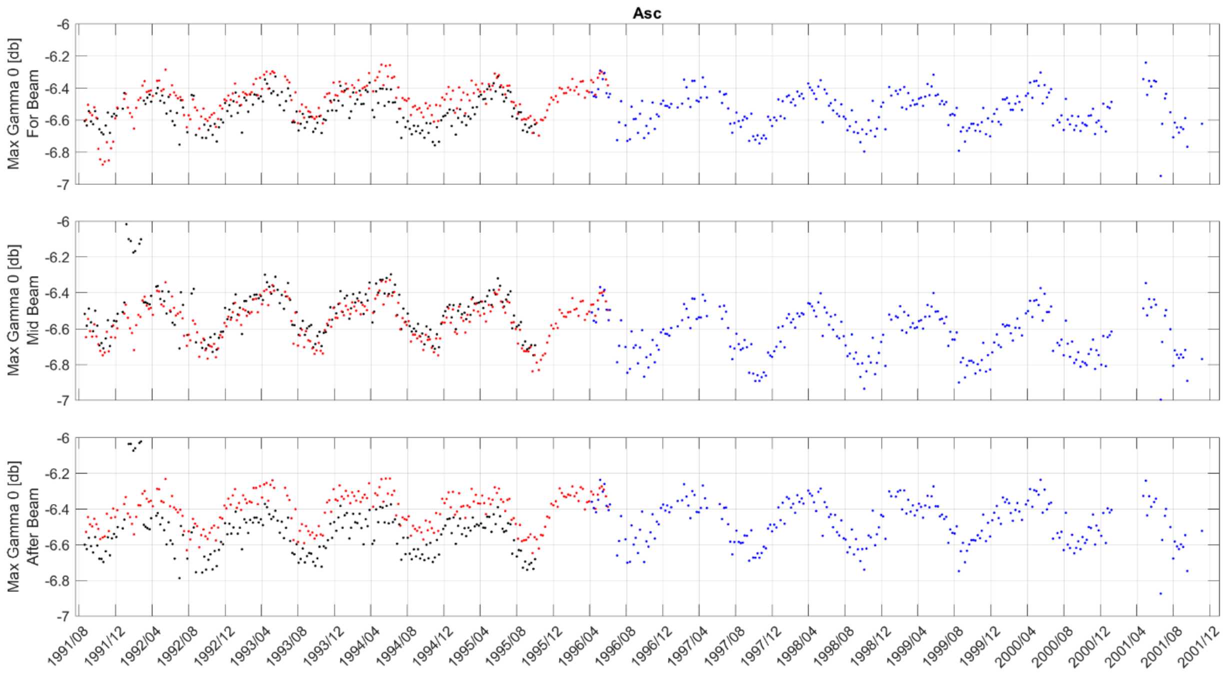

Figure 4 ERS1-OP (black), ERS1-ASPS reprocessed data (red) and ERS2-ASPS reprocessed data (blue) Scatterometer gamma-nought histogram peak position over the rain forest: weekly evolution of maximum position. From top to bottom For, Mid and After Beam. All statistics have been calculated considering only Ascending passes.

Figure 5 shows the evolution of the peak position for the Descending passes. The bias between ERS-1 operational and reprocessed data is clearly visible for the after Beam and in a lesser extent also in the Mid Beam. The periodic annual variation is also present with a smaller variability (about 0.4 dB). Moreover the peak values of the Mid antenna are confirmed to be lower (roughly 0.2 dB) than the fore-aft case. Finally in the period between April 1992 and December 1993 both ERS-1 data shows gaps in the data due to the frequent use over the target area of the SAR mode during this period.

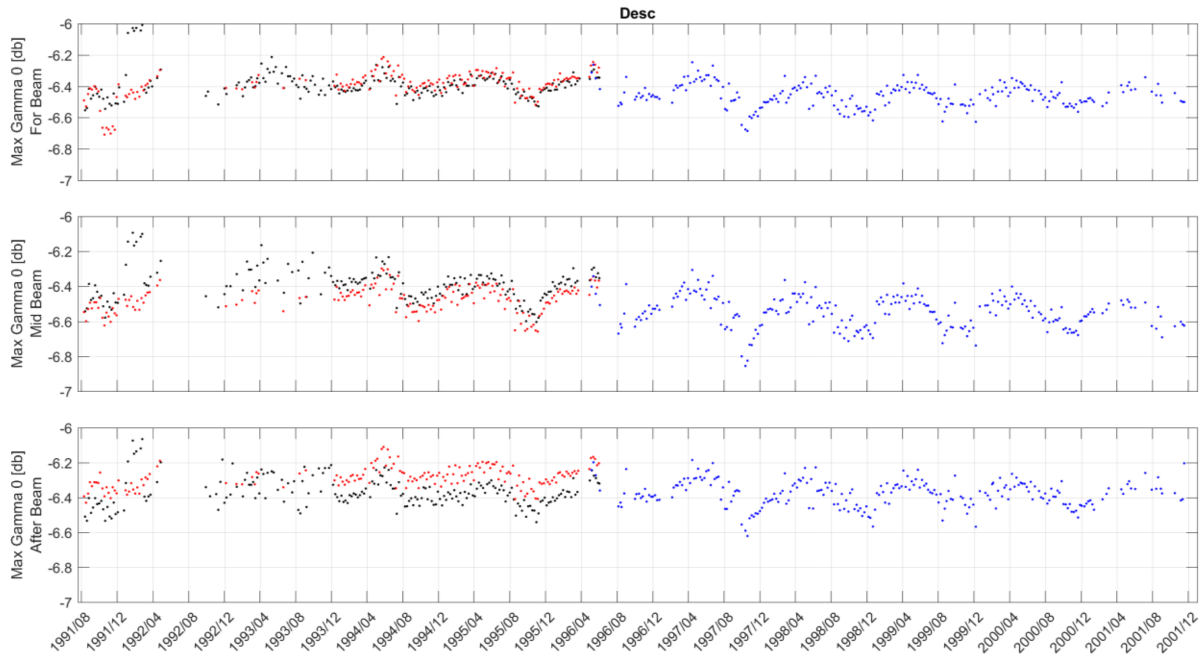

Figure 5 ERS1-OP (black), ERS1-ASPS reprocessed data (red) and ERS2-ASPS reprocessed data (blue) Scatterometer gamma-nought histogram peak position over the rain forest: weekly evolution of maximum position. From top to bottom For, Mid and After Beam. All statistics have been calculated considering only Descending passes.

Figure 6 shows the evolution of the standard deviation since the beginning of the mission. The ascending passes show a gamma nought standard deviation higher than the descending ones. No clear bias is present between the ERS-1 operational and ERS-1 ASPS reprocessed or ERS-2 reprocessed data. The data gap in the period between April 1992 and December 1993 in the descending passes causes the standard deviation of gamma nought to be higher and more variable due to a three days repeat cycle. The evolution of the gamma nought standard deviation is stable.

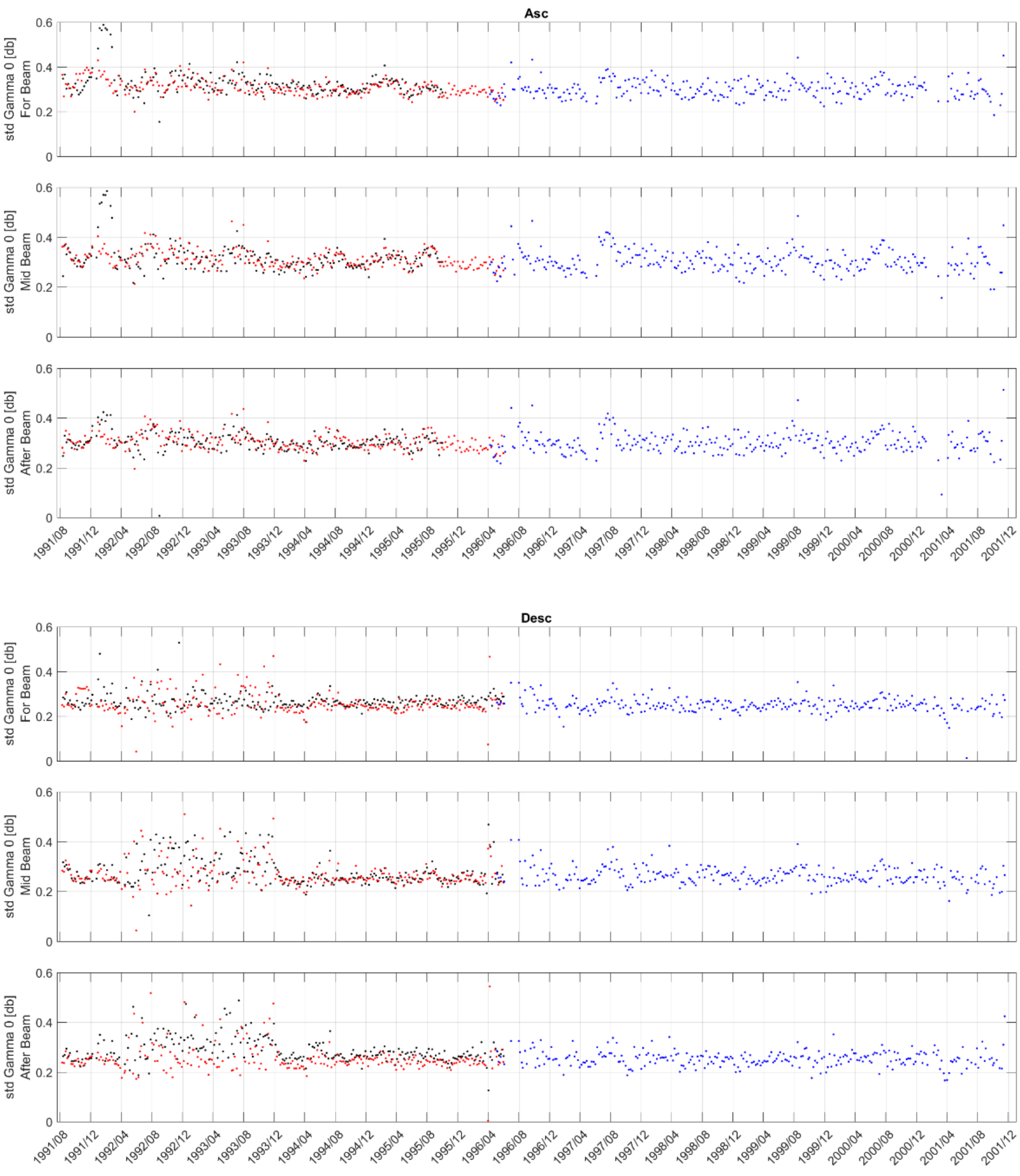

Figure 6 ERS1-OP (black), ERS1-ASPS reprocessed data (red) and ERS2-ASPS reprocessed data (blue) Scatterometer gamma-nought standard deviation histograms over the rain forest: weekly evolution of standard deviation. From top to bottom For, Mid and After Beam. Upper three plots ascending passes, lower three plots descending passes.

2.4 Antenna pattern: Gamma-nought as a function of incident angle

Error! Reference source not found. shows the antenna patterns as function of the incident angle for the full ERS-1 mission over the rain forest.

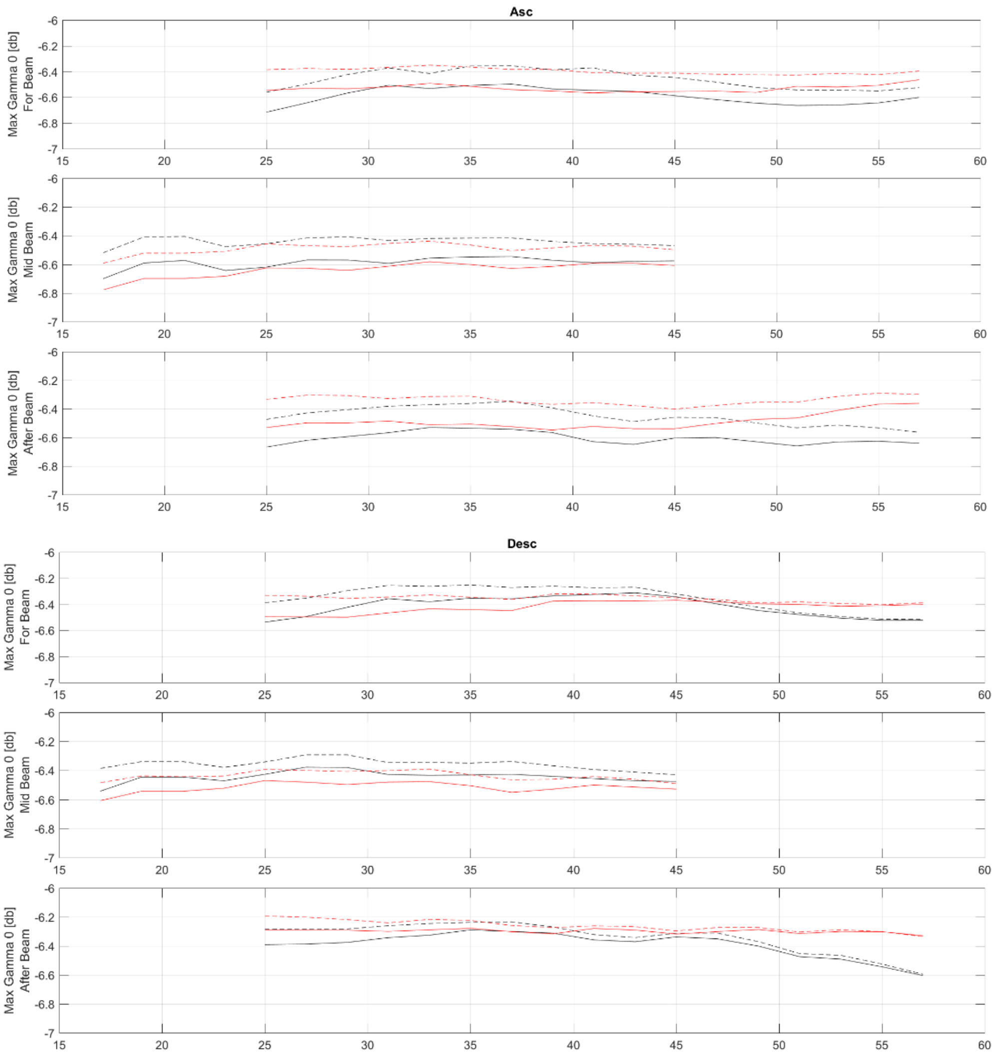

Figure 7 Antenna patterns as function of the incidence angle for the three beams: Descending passes, for ERS-1 Operational (back) ERS-1 reprocessed with ASPS (red). Continuous lines show the antenna pattern for the data between April and November (minimum of the Gamma nought), while dotted lines the data between December and May (maximum of the Gamma nought).

The antenna pattern have been analysed dividing the dataset between ascending and descending passes and as function of the month of the year considered: Months from December to May corresponding roughly to the period of maximum in the annual oscillation of the Gamma nought and April to November. The antenna patterns show a flat profile, within 0.3 dB, for both ascending and descending passes, the new reprocessing with ASPS have improved the stability of the antenna patterns in particular for the maximum curve and for the higher incidence angles, particularly clear for the for-aft beam in the descending passes. Some residual variation of the antenna pattern is still present for (smaller than 0.2 dB) for the mid beam and for the angle smaller than 25°.

3. INSTRUMENT PERFORMANCES

The instrument status is checked by monitoring the following parameters:

- **Centre of Gravity** and **standard deviation of the received signal spectrum**. This parameter is useful for the monitoring of the orbit stability, the performances of the Doppler compensation filter, the behaviour of the yaw steering mode and the performances of the devices in charge for the satellite attitude (e.g. gyroscopes, earth sensor).

- **Noise power I and Q channel**.

- **Internal calibration pulse power**.

The latter is an important parameter to monitor the transmitter and receiver chain, the evolution of pulse generator, the High Power Amplifier (HPA), the Travelling Wave Tube (TWT) and the receiver.

These parameters are extracted daily from the UWI products and averaged. The evolution of each parameter is characterised by a least square line fit. The coefficients of the line fit are printed in each plot.

3.1 Centre of gravity and standard deviation of received power spectrum

Figure 8 shows the evolution of the two parameters for each beam. The Centre of gravity (CoG) of the signal spectrum for the three antennae is very stable in the ERS-1 ASPS reprocessed data with a mean value very near to 0, these evidences the very good performances of the Doppler compensation filter. Moreover the standard deviation of the received spectrum is lower than the one of the operational ERS-1 data and very stable over the full mission.

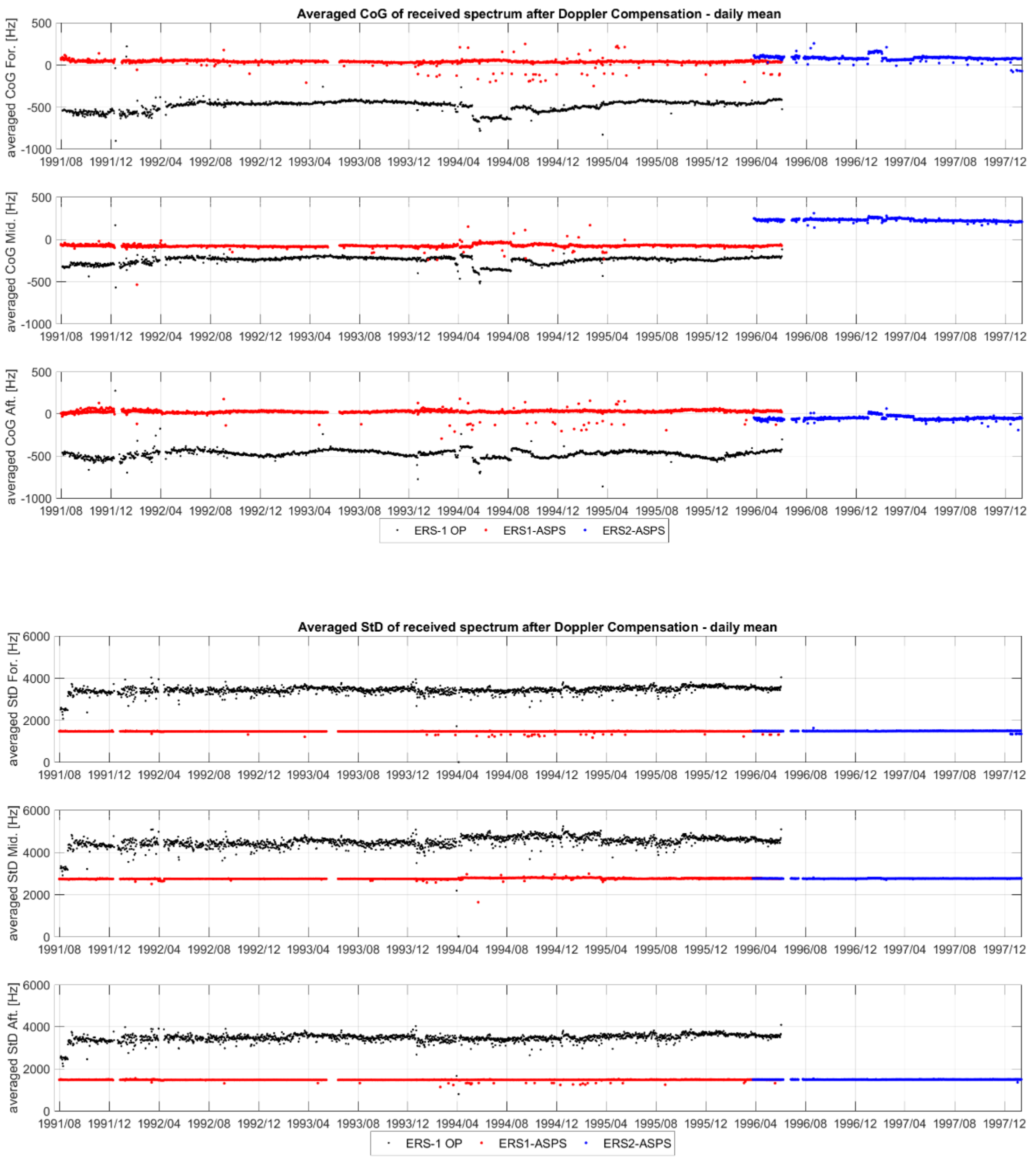

Figure 8 ERS1-OP (black), ERS1-ASPS reprocessed data (red) and ERS2-ASPS reprocessed data (blue) Scatterometer Centre of Gravity (top three panels) and standard deviation (bottom three panels) of received power spectrum for the three different beams (For, Mid and Aft)

3.2 Noise power level I and Q channel

The results of the monitoring are shown in Figure 9. The first set of three plots presents the noise power evolution for the I channel while the second set shows the Q channel. The noise level is less than 0.1 ADC Unit for all beams in the ASPS reprocessed ERS-1 data and it is always lower than the one in the operational dataset. A sharp increase in the noise level (both I and Q channels and for all the beams) is evident after May 1996 (near to the payload hibernation

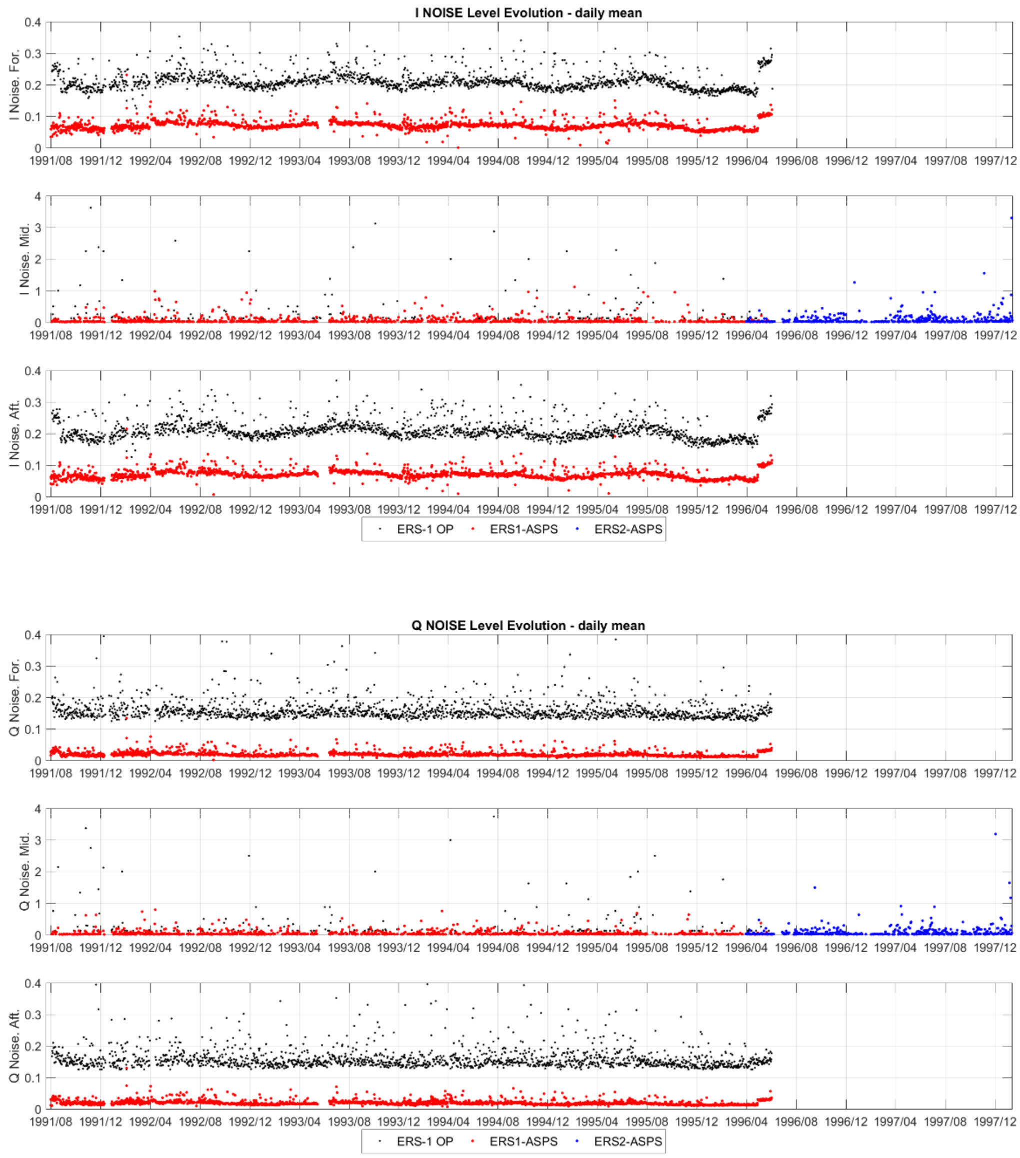

Figure 9 ERS1-OP (black), ERS1-ASPS reprocessed data (red) and ERS2-ASPS reprocessed data (blue) Scatterometer noise power I (top three panels) and Q channel (bottom three panels) for the three different beams (For, Mid and Aft). The ERS-2 data (blue) for For and Aft antennas are out the scale.

3.3 Power level of internal calibration pulse

For the internal calibration level, the results, since the beginning of the mission, are shown in Figure 10. The internal calibration level show no evident change between the ERS-1 ASPS reprocessed data and the operational data. The power level decrease since the beginning of the mission is confirmed. A sharp increase in the internal calibration power level after May 1996 is also evident.

Figure 10 ERS1-OP (black), ERS1-ASPS reprocessed data (red) and ERS2-ASPS reprocessed data (blue) Scatterometer power of internal calibration pulse for the three different beams (For, Mid and Aft).

4. PRODUCTS PERFORMANCES

The quality control analysis of the winds generated from the ASPS reprocessing is summarized in the plots of Figure 11; from top to bottom:

- the monitoring of the valid sigma-nought triplets per day.
- the comparison of the wind speed deviation: (bias and standard deviation per day) with the ECMWF forecast.
- the evolution of the wind direction quality. The ERS wind direction is compared with the ECMWF forecast. The plot shows the mean deviation per day.

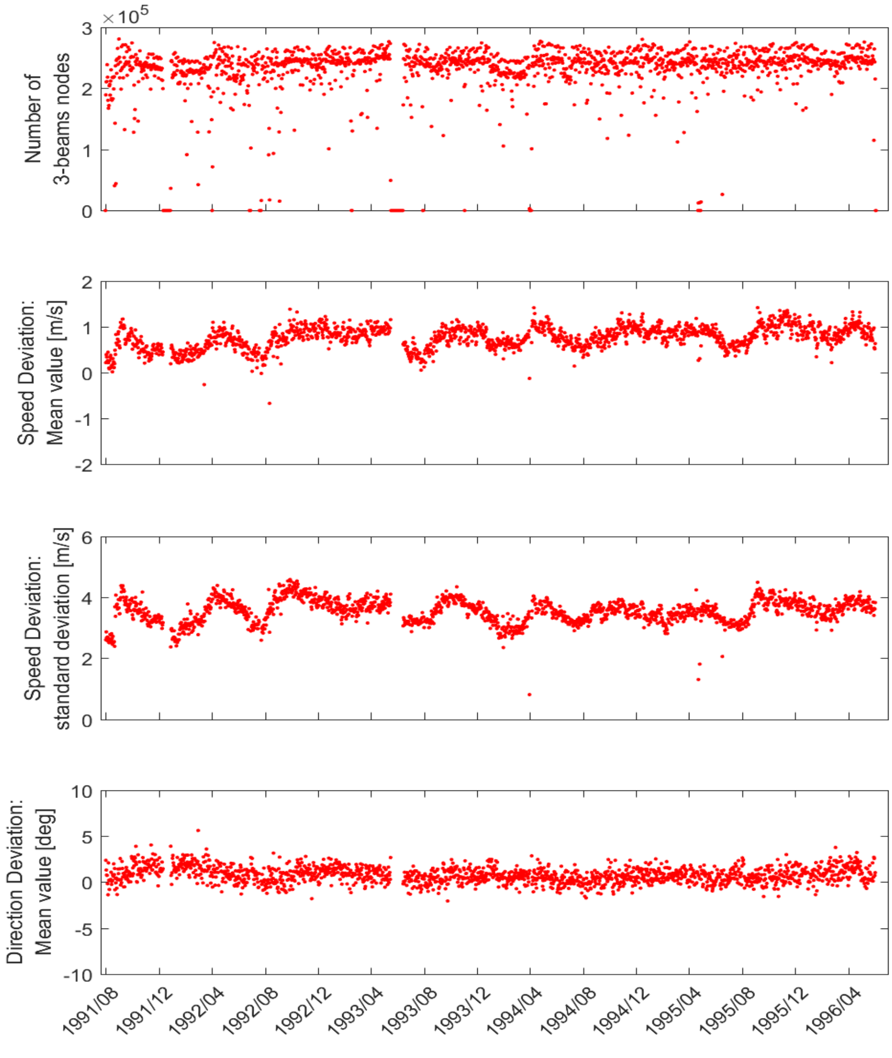

Figure 11 ERS-1 Scatterometer ASPS reprocessed data: wind products performance since the beginning of the mission.The results since the beginning of the mission can be summarized as a stable number of valid sigma- nought for the full mission, an accurate wind direction within ± 5. Wind speed shows an absolute bias of roughly 0.5 m/s and a standard deviation between 2 m/s and 4 m/s with respect to the ECMWF forecast. Both the mean and standard deviation have a seasonal pattern due to the different winds distribution between the winter and summer season.